J Mol Model (2012) 18:2633–2644
DOI 10.1007/s00894-011-1277-z

ORIGINAL PAPER

Conserved water-mediated H-bonding dynamics of catalytic His159 and Asp158: insight into a possible acid–base coupled mechanism in plant thiol protease

Tapas K. Nandi · Hridoy R. Bairagya · Bishnu P. Mukhopadhyay · Payel Mallik · Dipankar Sukul · Asim K. Bera

Received: 19 May 2010 / Accepted: 9 October 2011 / Published online: 9 November 2011

Abstract Cysteine protease is ubiquitous in nature. Excess activity of this enzyme causes intercellular proteolysis, muscle tissue degradation, etc. The role of water-mediated interactions in the stabilization of catalytically significant Asp158 and His159 was investigated by performing molecular dynamics simulation studies of 16 three-dimensional structures of plant thiol proteases. In the simulated structures, the hydrophilic W_1, W_2 and WD_1 centers form hydrogen bonds with the OD1 atom of Asp158 and the ND1 atom of His159. In the solvated structures, another water molecule, W_E, forms a hydrogen bond with the NE2 atom of His159. In the absence of the water molecule W_E, Trp177 (NE1) and Gln19 (NE2) directly interact with the NE2 atom of His159. All these hydrophilic centers (the locations of W_1, W_2, WD_1, and W_E) are conserved, and they play a critical role in the stabilization of His–Asp complexes. In the water dynamics of solvated structures, the water molecules W_1 and W_2 form a water... water hydrogen-bonded network with a few other water molecules. A few dynamical conformations or transition states involving direct (His159 ND1...Asp158 OD1) and water-mediated (His159 ND1...W_2...Asp158 OD1) hydrogen-bonded complexes are envisaged from these studies.

Keywords Plant thiol protease · Water dynamics · Catalytic His159–Asp158 · Acid–Base coupling

T. K. Nandi · H. R. Bairagya · B. P. Mukhopadhyay (✉) · P. Mallik · D. Sukul
Department of Chemistry, National Institute of Technology, Durgapur 713 209, India
e-mail: bpmk2@yahoo.com

A. K. Bera
Institute for Bioscience and Biotechnology Research, Rockville, MD 20850, USA

Introduction

Papain-like cysteine protease is a ubiquitous proteolytic enzyme that is present in a wide variety of living organisms, including plants [1]. Excess activity of this digestive enzyme results in the degradation of muscle tissue and intracellular proteolysis, etc. [2]. In recent times, cysteine protease has been considered a promising drug target for cancer, osteoporosis, and arthritis [3–5]. In addition, it is also being used in various industries, such as the leather processing and meat tenderization industries.

The catalytic residue His159 is located in an antiparallel β-sheet inside the deep active site cleft of the enzyme, and the catalytic residue Cys25 is positioned on the opposite side [6]. In plant thiol protease, the formation of the Cys25–His159 ion pair, the role of Asn175 in the catalytic triad, and the interactions of Gln19, Asp158, and Trp177 with His159 [7–9] are significant. To date, little work has been done on the involvement of water molecules in the stabilization of the thiolate–imidazolium ion pair [9, 10] and catalytic Asn175 [11]. The ionizable carboxyl side chain of Asp158 with His159 is significantly involved with the catalytic activity of papain [12], but detailed information on the role of water molecules in the coupling of the His–Asp ion pair is still unclear. In the double catalytic triads Cys25–His159–Asp158 and Cys25–His159–Asn175, the residues Asp158 and Asn175 have also been found to induce catalysis in papain [13, 14]. A comparison of the direct hydrogen-bonding interaction between the His (ND1) and Asp (OD1) (at a distance of ~2.3 Å) in the catalytic triad of serine protease [15] and the interaction between His159 (ND1) and Asp158 (OD1) (at a distance of ~5.6 Å) in

cysteine protease indicates the possibility of an alternative catalytic mechanism for plant cysteine protease. Again, considering the tautomeric forms of catalytic histidine in serine protease [16], we protonated the ND1 nitrogen atom of the imidazole ring in the catalytic histidine of cysteine protease and performed simulation. This study may shed some light on the direct or conserved water-mediated interactions and the stabilization of His159 through Asp158, as well as their manifestation in the catalytic mechanism of plant thiol protease.

Materials and methods

All of the X-ray crystal structures for plant thiol proteases were taken from the Protein Data Bank archive [17], and the corresponding parameters are included in Table 1. Only one molecule was present in the asymmetric unit of the crystal structures of 1PPN [18], 9PAP [19], 1PE6 [20], 1PPP [21], 1KHP [22], 1KHQ [22], 1BP4 [23], 1AEC [24], 2ACT [25], 1MEG [26], 1YAL [27], 1GEC [28], and 1IWD [29], whereas two molecules were present in the asymmetric unit of 2PNS [30]. In the other two structures, 1CQD [31] and 2BDZ (RCSB database, 2005), the enzyme crystallized as a tetramer.

Structure preparation

During the analysis, only the apo forms of the protein structures were considered. Small molecules bound to the protein structures were then removed. However, for the dimeric (2PNS) and tetrameric (1CQD and 2BDZ) structures, the protein chain containing the highest number of water molecules was selected and separated using the Swiss-PdbViewer program [32].

Molecular dynamics simulations of the X-ray structure containing water molecules

The sixteen structures (PDB) of plant thiol protease were used in molecular dynamics (MD) simulation studies. Before starting the simulation, each structure (including the crystal water molecules) was converted to its Protein Structure File (PSF) using the automatic PSF generation plug-in tool v.1.2 within the Visual Molecular Dynamics v.1.8.6 program [33]. The catalytic residue His159 was protonated at the ND1 atom of the imidazole group (to convert it into its HSD form), and the TIP3P water model was employed for all crystal water molecules. After that, each respective PSF structure was initially energy minimized (1000 cycles to eliminate initial contacts that would

Table 1 Preliminary X-ray structural data for the plant thiol proteases

PDB Code (year deposited)	Resolution (Å)	*R* factor	Residue no. in catalytic triad			No. of water molecules	Ligand	Reference
			C	H	N			
1PPN* (1991)	1.60	0.16	25	159	175	226	C25 with bound atom	18
9PAP (1986)	1.65	0.161	25	159	175	195	C25 in oxidized form	19
1PE6 (1991)	2.10	0.159	25	159	175	181	E64C	20
1PPP (1993)	1.90	0.194	25	159	175	205	E64C	21
1KHP (2001)	2.00	0.185	25	159	175	53	GLM	22
1KHQ (2001)	1.60	0.149	25	159	175	105	GLM	22
1BP4 (1998)	2.20	0.190	25	159	175	88	ALD	23
1AEC (1992)	1.86	0.145	25	162	182	268	E64	24
2ACT (1979)	1.70	0.171	25	162	182	272	Mature peptidase	25
1MEG (1996)	2.00	0.193	25	159	179	94	E64	26
1YAL (1996)	1.70	0.192	25	159	179	222	Mature peptidase	27
1CQD (1999)	2.10	0.213	27	161	181	95 (chain A)	THJ	31
1IWD (2002)	1.63	0.161	25	158	178	208	THJ (mature)	29
2BDZ (2005)	2.10	0.177	25	159	175	108 (chain A)	E64	Gavira et al., 2005 RCSB Database,
1GEC (1995)	2.10	0.196	25	159	179	117	Benzoxycarbonyl Leu-Val-Gly-methylene bound to C25	28
2PNS (2007)	1.90	0.173	25	157	173	131 (Chain-B)	THJ (mature)	30

* 1PPN was used as the template structure

destabilize the system) using the CHARMM22 force field [34]. Then all of the structures (with crystal water molecules) were simulated using Auto Interactive Molecular Dynamics (AutoIMD), which links the visualization program Visual Molecular Dynamics v.1.8.6 with the molecular dynamics program Nanoscale Molecular Dynamics (NAMD) v.2.6 [35, 36]. MD simulations were performed for every structure by selecting a 10 Å zone around the catalytic center of the enzyme for the molten zone of AutoIMD (where the catalytic triad and other potential residues with water molecules were simulated), and the rest of the enzyme was considered a fixed zone of AutoIMD. MD simulations were performed for all of the structures up to 2 ns at a temperature of 300 K with a time step of 2 fs by means of Langevin dynamics using the CHARMM22 force field with exclude scaled 1–4 (so that the 1–2, 1–3 and 1–4 atom pairs were excluded from non-bonded interactions), and the distance cutoff was 10 Å, which relaxed the water molecules and propagated them towards the structural equilibrium position. The fluctuations in potential energy, kinetic energy, and total energy were monitored. The plots of potential energy and kinetic energy against time at constant temperature revealed that the equilibrium was closed when the average potential energy and kinetic energy were constant. The simulations adequately converged within 1 ns. Different snapshots were taken every 200 ps during the 2 ns simulation.

Molecular dynamics simulations of solvated structures

To realize a detailed investigation of the water molecules, we performed MD simulation studies after solvating the template 1PPN structure. We solvated the protein in two ways: using the Visual Molecular Dynamics (VMD) and Conditional Hydrophobic Accessible Surface Area (CHASA) programs.

In procedure I, the apo form of 1PPN was placed into a periodic box and solvated with 9042 TIP3P water molecules (which were located to 12 Å from the protein), and the PSF file of the solvated 1PPN was generated using the automatic PSF generation plug-in tool v.1.2 in the VMD v.1.8.6 program, using the CHARMM22 force field. The system (containing water molecules) was then energy minimized for 1000 steps while keeping the protein fixed, using the NAMD v. 2.6 program. In the next step, the structure was again energy minimized for 2000 steps (where both the protein and water molecules were included), and was simulated at 300 K. After reaching the system equilibrium, water dynamics was performed for 2 ns, where water molecules within 5 Å of the protein surface were allowed to move.

In procedure II, the protein was solvated using the CHASA program [37]. During solvation, a probe radius of 1.4 Å was used, and the O (oxygen) atom of the water molecule was placed 2.95 Å from the backbone N (nitrogen) and O (oxygen) atoms of the protein molecule [38, 39]. Further, we performed MD simulation on the solvated 1PPN structure for up to 2 ns with the CHARMM22 force field. All of the atoms of both the protein and the water were allowed to move during the entire simulation process. Snapshots were taken every 100 ps to monitor the different interactions of the water molecules with the important residues involved in the catalytic process.

Stability free energy

The stability free energy was calculated for all of the PDB and MD-simulated structures (including the crystal water molecules) using the program FOLDX [40]. The temperature, ionic strength, pH, and vdW parameters were assigned values of 300 K, 0.05 (M), 7.0, and 2.0 Å, respectively.

Identification of the conserved water-mediated interaction sites

The conserved water-mediated interaction sites of the plant thiol protease (in all of the X-ray and MD-simulated apo structures) were identified using the standard least-square fitting algorithm in the Swiss-PdbViewer program. The three-dimensional structure of 1PPN was taken as the template/reference structure, and the remaining three-dimensional structures were superposed on the backbone atoms of the template structure. The RMSD values were found to be ~0.28–0.75 Å. After the superposition had been performed, the conserved water-mediated interaction sites were identified by comparing the superposed structures. Water molecules found to lie within 1.5 Å [41] were taken to be conserved.

Results and discussion

During the simulation (Table 1), we recorded snapshots at different time intervals and investigated the water-mediated interactions around the NE2 and ND1 nitrogen atoms of catalytic His159 and the carboxyl oxygen atoms of Asp158.

In most of the three-dimensional structures of inhibitor-bound plant thiol protease (Fig. 1), the backbone N_b atom of catalytic histidine (His159) is hydrogen bonded to the O_b atom of the corresponding residues in the β-sheet and the carboxyl OD1 oxygen of Asp158 (or OE1 of Glu158 in 1MEG, and to OD1 of Asp161 in the 1AEC and 2ACT structures). However, in 1CQD, 1IWD, and 2PNS (using their PDB ids), the N_b atom of catalytic histidine is hydrogen bonded to the OD1 oxygen of the nearby Asn residue. In the X-ray crystal structures, the distance between the side-chain carboxyl OD1 of Asp158 and

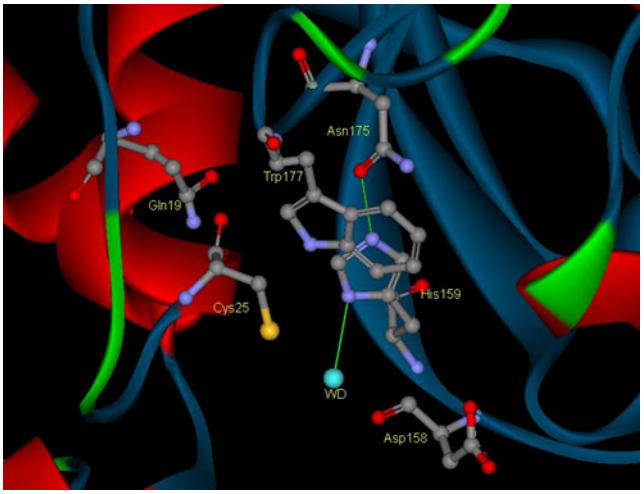

Fig. 1 Important residues at the active site of plant thiol protease, and the conserved water molecules (WD)

ND1 of catalytic His159 is ~5.6 Å, and the NE2 atom is hydrogen bonded to the OD1 amide oxygen atom (2.55–2.89 Å) of the catalytic Asn175 residue. In 1PPN, 9PAP, 1KHQ, and 2ACT (using their PDB ids), two conserved water molecules WD_1 and WD_2 are observed to form hydrogen bonds (bond lengths: ~3.0–3.5 Å and ~4.0 Å) with ND1 of the catalytic histidine. On the other hand, in the remaining structures, oxygen or some other potential atom of the inhibitor (E64C, aldehyde inhibitor, E64, diazomethylketone inhibitor, and thiosulfate) occupies the WD_1 and WD_2 positions and forms hydrogen bonds (~2.88–3.29 Å) with the ND1 atom (Table 2). In the case of 2ACT, the "SG" atom of Cys25 interacts directly with ND1 (~3.30 Å) of His162. Table 2 and Fig. 2 (I) illustrate the interactions between different amino acid residues and water molecules in the X-ray crystal structures. In most inhibitor-bound complexes, the carboxyl OD1 atom of Asp158 forms a hydrogen bond with the water molecule W_1 (bond length: ~3.2 Å), and this hydrophilic site was found to be conserved in all of the structures (Fig. 2(I)).

During the simulation of all of the three-dimensional structures (within 1–20 ps), the hydrogen-bonding interaction NE2 (His159)...OD1 (Asn175) disappeared and the water molecule W_E formed a hydrogen bond with the NE2 atom (~2.77–3.06 Å). However, after 800, 600, and 800 ps simulations of 1PPP, 1KHP, and 1AEC (using their PDB ids), the NE2-bound water molecule (W_E) migrates from this site and the side chains of Trp177 [42] and Gln19 interact with the NE2 atom (Fig. 2 and 3). The distances between the NE2 atom (of catalytic histidine) and the water molecule (W_E), the Trp177 (NE1) residue, and the Gln19 (NE2) residue at different phases of the simulation are included in Table 2. Throughout the dynamics of 1PE6, 1KHQ, 1BP4, 2ACT, 1MEG, 2BDZ, 1CQD, 1YAL, 2PNS, 1GEC, and 1IWD (using their PDB ids), no water molecule is observed to form a hydrogen bond with NE2. However, this nitrogen atom seems to be stabilized by the side chains of the Trp177 and Gln19 residues, which are shown in Table 2 and Fig. 2 (II and III). During simulation, the hydrogen-bond distances between the ND1 atom of His159 and the water molecules WD_1 and WD_2 are observed to be elongated (compared to their initial lengths in the X-ray structures), and ultimately both the water molecules migrate from the sites (by breaking the hydrogen bond with ND1), while the carboxyl OD1 atom of Asp158 simultaneously approaches that nitrogen atom and interacts directly with ND1, as shown in Fig. 2 (II^I). In some cases, the OD1 atom occupies the WD_1 conserved hydrophilic water site. For 1PPN, 9PAP, 1PPP, 1KHP, and 1AEC (using their PDB ids), the ND1-bound conserved water molecule WD_1 is replaced by the OD1 atom of Asp158, and the His–Asp pair is stabilized through a direct ND1–OD1 hydrogen-bonding interaction. However, in 9PAP, 1PE6, 1KHQ, 1BP4, 1IWD, and 1GEC (using their PDB ids), another water molecule W_2 appears to occupy a conserved hydrophilic site, which seems to be different from the previous WD_2 position. The W_2 center forms a hydrogen bond with the carboxyl oxygen atom of aspartic acid and ultimately bridges the ND1 atom to OD1 (Asp158) through the water molecule OD1 (Asp158)...W2...ND1 (His159), as shown in Fig. 2 (III). The water molecules occupy these three conserved hydrophilic sites (WD_1, W_1, and W_2) in the different simulated structures of plant thiol protease. Thus, the stabilization of the catalytic acid–base pair through direct Asp158...(ND1)–His159–(NE2)...W or water-mediated Asp158...W...(ND1)–His159–(NE2) processes appears to be interesting in plant thiol protease. This kind of water–imidazole interaction has been found to be energetically favorable in different protein structures [43]. However, due to the high stability of the acid–base coupled interaction between the catalytic His159 and Asp158 residues, the residence occupancy/frequency of dynamic conformation II^I (Fig. 2) is high in 1PPN, 9PAP, 1KHP, and 1AEC.

No such water-mediated or direct recognition of His... Asp residues is observed for 2ACT, 1MEG, and 2BDZ (using their PDB ids), which may be due to the different orientations of their side chains and the variation in torsion angles. The His159 (ND1) is found to interact with the O_b atom of the respective Ala163 (in 2ACT) or Ala160 (1MEG and 2BDZ), and the ND1...O_b distances are given in Table 2. The changes in the χ_1 and χ_2 torsional angle values for the catalytic His and Asp/Asn residues are given in Table 3. Such variations in the torsion angles of catalytic histidine have also been observed during the dynamics of other thiol protease structures [44]. The durations of the various intermediate/dynamical conformations I–III (as shown in Fig. 2 and 3), involving interactions of residues,

Table 2 Interactions of water molecules and different residues with the NE2 and ND1 atoms of the imidazole ring of catalytic histidine in the X-ray and MD-simulated structures

PDB structures/ NE2 and ND1 atoms of catalytic histidine		X-ray structure (distance in Å)	MD-simulated structure in ns (all the distances, in Å, of the respective atoms/residues from the NE2 and ND1 atoms are given in parentheses)									
			0.2	0.4	0.6	0.8	1.0	1.2	1.4	1.6	1.8	2.0
1PPN	NE2	Asn175 OD1 (2.55)	W317 (3.06)	W317 (2.90)	W317 (2.77)	W317 (2.89)	W317 (2.84)	W317 (3.03)	W317 (2.79)	W317 (2.83)	W317 (2.80)	W317 (3.00)
	ND1	W401 (3.40)	R_D (3.08)	R_D (2.90)	R_D (2.81)	R_D (2.64)	R_D (2.73)	R_D (2.63)	R_D (2.81)	R_D (2.94)	R_D (2.91)	R_D (2.79)
9PAP	NE2	Asn175 OD1 (2.77)	W42 (2.92)	W42 (2.70)	W42 (2.70)	W42 (2.82)	W42 (2.94)	W42 (2.87)	W42 (2.85)	W42 (2.89)	W42 (3.07)	W42(2.95)
	ND1	W42 (3.05)	R_D (3.31)	R_D (3.10)	R_D (2.93)	R_D (3.21)	R_D (3.45)	R_D (2.97)	R_D (3.08)	R_D (3.02)	R_D (2.95)	R_D (2.78)
1PPP	NE2	Asn175 OD1 (2.82)	W287 (2.70)	W287 (3.13)	W287 (3.30)	W287 (3.04)	– R_W/R_Q (3.22)/(2.96)	– R_W/R_Q (3.07)/ (3.15)	– R_W/R_Q (3.33)/ (3.72)	– R_W/R_Q (3.18)/ (3.03)	– R_W/R_Q (3.15)/ (3.07)	– R_W/R_Q (3.66)/ (3.29)
	ND1	E6C O18 (2.94)	R_D (3.78)	R_D (2.96)	R_D (2.96)	R_D (3.31)	R_D (4.16)	R_D (4.70)	R_D (4.31)	R_D (3.84)	R_D (4.51)	R_D (3.90)
1KHP	NE2	Asn175 OD1 (2.81)	W317 (3.16)	W317 (2.84)	– R_W/R_Q (3.15)/ (4.00)	– R_W/R_Q (3.18)/ (3.08)	– R_W/R_Q (3.26)/(4.60)	– R_W/R_Q (3.27)/ (3.45)	W317 (2.86)	– R_W/R_Q (3.48)/ (5.28)	W317 (2.92)	W317 (3.02)
	ND1	GLM 253 CM (3.15)	R_D (2.98)	R_D (2.76)	R_D (3.52)	R_D (3.69)	R_D (2.64)	R_D (3.26)	R_D (3.10)	R_D (2.97)	R_D (3.10)	R_D (2.72)
1AEC	NE2	Asn175 OD1 (2.88)	W220 (2.88) W582 (3.00)	W220 (2.86) W582 (2.83)	W220 (2.98) W582 (3.29)	W129 (3.46)	– R_W/R_Q(2.81)/ (2.91)	–R_W/R_Q (3.00)/ (2.91)	– R_W/R_Q (2.99)/ (2.89)	– R_W/R_Q (3.06)/ (2.99)	W193 (2.73)	W193 (2.80)
	ND1	W215 (3.48)	R_D (3.02)	R_D (2.65)	R_D (2.87)	W215 (3.05)	W215 (2.99)	–	W215 (3.04)	W220 (3.39)	R_D (2.75)	R_D (2.89)
1PE6	NE2	Asn175 OD1 (2.74)	– R_W/R_Q (3.22)/ (2.96)	– R_W/R_Q 2.95)/ (3.33)	– R_W/R_Q 3.43)/ (3.13)	– R_W/R_Q 3.43)/ (3.12)	– R_W/R_Q 2.94)/ (3.04)	– R_W/R_Q 3.19)/ (3.09)	– R_W/R_Q 3.07)/ (3.70)	– R_W/R_Q 3.51)/ (3.80)	– R_W/R_Q 3.15)/ (3.20)	– R_W/R_Q 3.81)/ (3.10)
	ND1	W234 (3.33)	W234 (3.05)	W234 (2.95)	W234 (2.81)	W234 (3.29)	W234 (2.90)	W234 (3.00)	W234 (2.94)	W234 (2.91)	W234 (2.76)	W234 (3.58)
1KHQ	NE2	Asn175 OD1 (2.80)	– R_W/R_Q (3.10)/(2.94)	– R_W/R_Q (2.98)/ (3.21)	–R_W/R_Q (2.88)/ (3.10)	–R_W/R_Q (4.11)/ (3.08)	– R_W/R_Q (3.09)/ (3.23)	–R_W/R_Q (2.99)/ (3.29)	– R_W/R_Q (3.06)/ (3.11)	– R_W/R_Q (3.51)/ (3.10)	– R_W/R_Q (3.39)/ (3.41)	– R_W/R_Q (3.03)/ (2.97)
	ND1	W350 (3.31)	W379 (2.88)	W379 (3.20)	W379 (3.26)	W379 (3.20)	W379 (2.85)	W379 (2.97)	W379 (2.96)	W379 (2.90)	W379 (2.83)	W379 (2.99)
1BP4	NE2	Asn175 OD1 (2.80)	– R_W/R_Q (3.04)/(3.05)	– R_W/R_Q (3.26)/ (3.04)	– R_W/R_Q (2.93)/ (3.26)	– R_W/R_Q (3.00)/ (3.01)	– R_W/R_Q (2.89)/ (3.04)	– R_W/R_Q (3.29)/ (3.20)	– R_W/R_Q (2.97)/ (2.91)	– R_W/R_Q(3.12)/ (3.43)	– R_W/R_Q (3.10)/ (3.19)	– R_W/R_Q (3.04)/ (3.26)
	ND1	ALD 213 O34 (2.95)	W412 (3.70)	W412 (2.80)	W412 (2.93)	W412 (3.20)	W412 (2.87)	W412 (3.04)	W412 (3.14)	W412 (3.20)	W412 (3.25)	W412 (3.19)
2ACT	NE2	Asn175 OD1 (2.79)	– R_W/R_Q (4.14)/(2.96)	– R_W/R_Q (3.90)/ (5.81)	–R_W/R_Q (3.39)/ (2.49)	– R_W/R_Q(2.85)/ (2.86)	– R_W/R_Q (2.89)/ (3.05)	– R_W/R_Q (2.91)/ (2.78)	– R_W/R_Q (3.01)/ (3.01)	– R_W/R_Q (3.37)/ (3.01)	– R_W/R_Q (3.04)/ (3.14)	– R_W/R_Q (2.86)/ (3.15)
	ND1	Cys25 SG (3.30)	R_A (4.76)	R_A (4.36)	R_A (2.81)	R_A (5.18)	R_A (3.96)	R_A (3.38)	R_A (3.40)	R_A (3.84)	R_A (3.33)	R_A (3.82)
1MEG	NE2	Asn175 OD1 (2.68)	– R_W/R_Q (3.16)/(3.39)	– R_W/R_Q (3.17)/ (3.39)	– R_W/R_Q (2.77)/ (3.01)	– R_W/R_Q (2.90)/ (3.28)	– R_W/R_Q (3.25)/ (3.05)	– R_W/R_Q (2.87)/ (3.22)	– R_W/R_Q (3.10)/ (3.00)	– R_W/R_Q (3.01)/ (3.11)	– R_W/R_Q (3.17)/ (3.10)	– R_W/R_Q (3.16)/ (3.16)
	ND1	E64 217 O1 (2.88)	R_A (3.49)	R_A(3.28)	R_A (2.85)	R_A(3.04)	R_A (2.92)	R_A(3.10)	R_A (3.24)	R_A(3.27)	R_A (3.17)	R_A (3.25)
2BDZ (chain A)	NE2	Asn175 OD1 (2.77)	– R_W/R_Q (2.93)/(3.34)	– R_W/R_Q (3.02)/ (3.3)	– R_W/R_Q (2.97)/ (2.94)	– R_W/R_Q (2.93)/ (3.02)	– R_W/R_Q (2.81)/ (3.06)	– R_W/R_Q (2.77)/ (3.01)	– R_W/R_Q (2.90)/ (3.14)	– R_W/R_Q (2.86)/ (2.96)	– R_W/R_Q (3.06)/ (3.22)	– R_W/R_Q (3.08)/ (2.73)
	ND1	W1132 (3.54) E64 501 O2 (3.29)	R_A (2.89)	R_A (3.29)	R_A (3.48)	R_A (3.14) Asn 175 OD1 (3.33)	R_A (3.27)	R_A (3.57)	R_A (2.96)	R_A (3.06)	R_A (2.94)	R_A (2.83)
1CQD (chain A)	NE2	Asn181 OD1 (2.79)	– R_W/R_Q (3.02)/(3.67)	– R_W/R_Q (3.15)/ (3.90)	– R_W/R_Q (3.27)/ (3.35)	– R_W/R_Q (2.92)/ (3.79)	– R_W/R_Q (2.93)/ (3.76)	– R_W/R_Q (2.91)/ (4.05)	– R_W/R_Q (2.96)/ (3.63)	– R_W/R_Q (2.99)/ (3.38)	– R_W/R_Q (3.05)/ (3.81)	– R_W/R_Q (2.87)/ (3.68)
	ND1	THJ 800 S2 (3.00)	R_N (2.61)	R_N (2.84)	R_N(2.96)	R_N (2.82)	R_N (2.85)	R_N (2.75)	R_N (2.76)	R_N (2.87)	R_N (2.83)	R_N (2.96)
1YAL	NE2	Asn179 OD1	– R_W/R_Q	– R_W/R_Q (2.94)/	– R_W/R_Q (3.18)/	– R_W/R_Q (3.01)/	– R_W/R_Q (2.94)/	– R_W/R_Q (2.89)/	– R_W/R_Q (3.49)/	– R_W/R_Q (3.22)/	– R_W/R_Q (3.05)/	– R_W/R_Q (3.01)/

Table 2 (continued)

PDB structures/ NE2 and ND1 atoms of catalytic histidine		X-ray structure (distance in Å)	MD-simulated structure in ns (all the distances, in Å, of the respective atoms/residues from the NE2 and ND1 atoms are given in parentheses)									
			0.2	0.4	0.6	0.8	1.0	1.2	1.4	1.6	1.8	2.0
		(2.81)	(3.03)/(3.16)	(3.27)	(3.24)	(3.09)	(3.31)	(3.03)	(3.18)	(3.12)	(3.25)	(3.30)
	ND1	SCH25 CB (3.48)	$R_D(O_b)$ (2.83)	$R_D(O_b)$ (2.93)	$R_D(O_b)$ (2.79)	$R_D(O_b)$ (3.02)	$R_D(O_b)$ (2.89)	$R_D(O_b)$ (3.10)	$R_D(O_b)$ (2.71)	$R_D(O_b)$ (2.65)	$R_D(O_b)$ (2.81)	$R_D(O_b)$ (2.75)
2PNS (chain B)	NE2	Asn173 OD1 (2.89)	– R_W/R_Q (3.10)/(3.20)	– R_W/R_Q (3.03)/ (3.16)	– R_W/R_Q (3.10)/ (3.42)	– R_W/R_Q (3.02)/ (3.67)	– R_W/R_Q (3.14)/ (3.01)	– R_W/R_Q (2.83)/(3.02)	– R_W/R_Q (2.93)/ (3.29)	– R_W/R_Q (3.53)/ (3.19)	– R_W/R_Q (3.39)/ (3.53)	– R_W/R_Q (3.20)/ (3.33)
	ND1	W720 (3.35) THJ 602 O1 (3.04)	–	–	–	–	–	Cys25 SG (3.49)	R_N (3.35)	R_N (3.05)	R_N (2.83)	R_N (2.98)
1GEC	NE2	Asn179 OD1 (2.79)	– R_W/R_Q (2.97)/(2.87)	– R_W/R_Q (3.18)/ (3.01)	– R_W/R_Q (3.47)/ (2.98)	– R_W/R_Q (3.20)/ (3.01)	– R_W/R_Q (3.00)/ (3.12)	– R_W/R_Q (3.39)/ (3.20)	– R_W/R_Q (3.17)/ (3.15)	– R_W/R_Q (3.03)/ (2.97)	– R_W/R_Q (2.95)/ (3.02)	– R_W/R_Q (3.15)/ (3.08)
	ND1	W235 (3.49)	R_S (3.29)	R_S (3.61)	R_S (3.83)	R_S (3.34)	R_S (3.61)	R_S (3.61)	R_S (3.67) W235 (3.49)	R_S (3.30)	R_S (3.40)	R_S (3.58)
1IWD	NE2	Asn178 OD1 (2.80)	– R_W/R_Q (3.02)/(3.06)	– R_W/R_Q (3.25)/ (3.04)	– R_W/R_Q (3.24)/ (3.14)	– R_W/R_Q (3.24)/ (3.11)	– R_W/R_Q (2.93)/ (3.12)	– R_W/R_Q (2.98)/ (3.26)	– R_W/R_Q (2.98)/ (3.26)	– R_W/R_Q (2.96)/ (3.20)	– R_W/R_Q (3.07)/ (3.39)	– R_W/R_Q (3.06)/ (2.90)
	ND1	W442 (3.25)	R_N (3.38)	R_N (3.12)	R_N (3.25)	R_N (2.83)	R_N (3.08)	R_N (2.95)	R_N (2.95)	R_N (3.04)	R_N (3.41)	R_N (3.10)
			W486 (3.06)	W508 (3.24)	W508 (3.06)	W442 (3.24)	W442 (3.13)			W442 (2.97)		W486(2.95)

R_D OD1 atom of Asp158 (1PPN, 9PAP, 1PPP, 1KHP)/Asp161 (1AEC)

R_Q NE2 atom of Gln19 (In all structures)

R_D (O_b) backbone oxygen atom of Asp158;

R_Q NE2 atom of Gln19 (in all structures)/Gln21 (1CQD)

R_N backbone oxygen atom of Asn160 (1CQD)/Asn156 (2PNS)/Asn157 (1IWD)

R_W NE1 atom of Trp177 (1PPN, 9PAP, 1PPP, 1KHP, 1PE6, 1KHQ, 1BP4, 2BDZ)/Trp184 (1AEC, 2ACT)/Trp181 (1MEG, 1YAL, 1GEC)/Trp183 (1CQD)/Trp175 (2PNS)/Trp180 (1IWD)

R_A backbone oxygen atom of Ala160 (1MEG, 2BDZ)/Ala163 (2ACT)

R_S Ser136 (OG atom)

E6C N-[1-hydroxycarboxyethyl-carbonyl] lucylamino-2-methylbutane

GLM 1-aminopropan-2-one of the ligand Ley-Phe-Glm

ALD carbobenzyloxyleucinyl-leuciny-leucinal

E64 N-[*N*-[1-hydroxycarboxyethylcarbonyl] leucylaminobutyl] guanidine

THJ thiosulfate

SCH thiomethylated cysteine

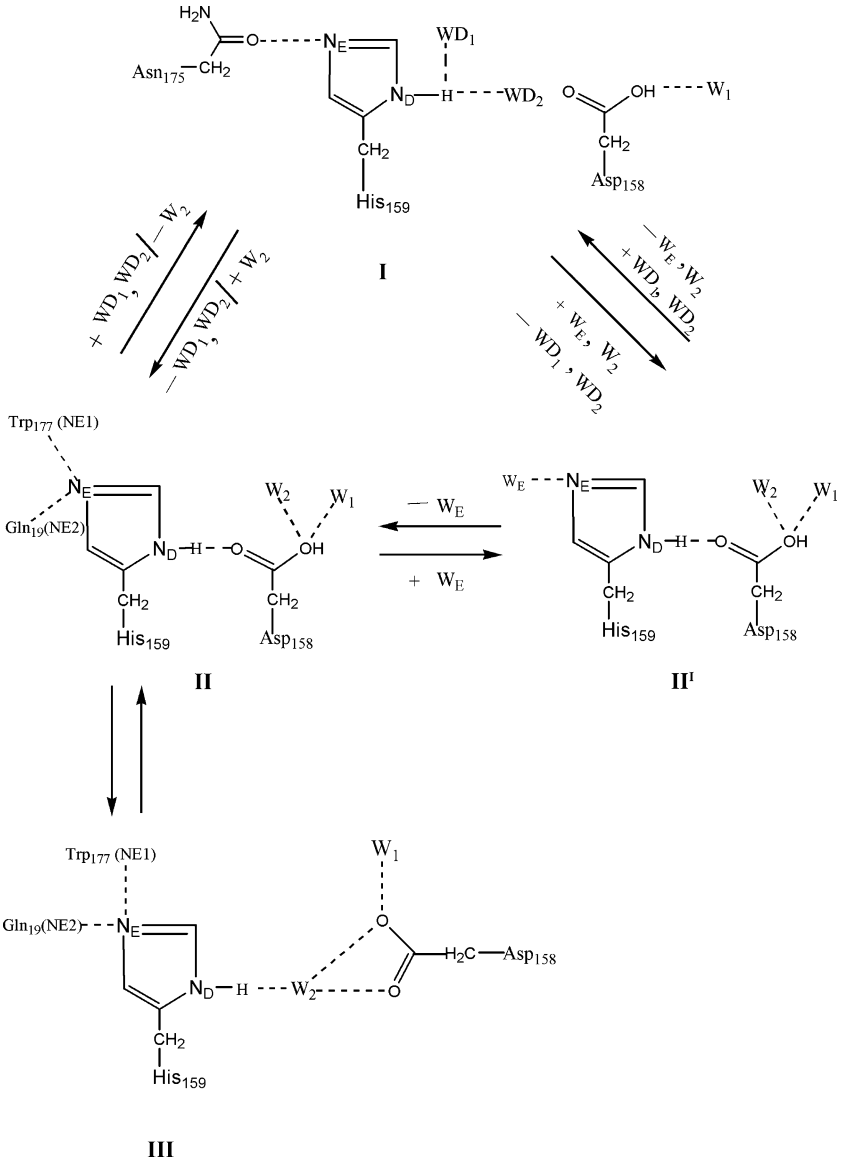

Fig. 2 Interactions of important residues and water molecules (W_E and WD) with the imidazole ring of catalytic histidine in X-ray (*I*) and other intermediate (*II–III*) structures (obtained during MD simulation). The interactions are shown by *broken lines*

water molecules, or conserved hydrophilic centers with catalytic histidine (in the different unliganded X-ray and MD-simulated structures of plant cysteine protease), are summarized in Table 4. The stability free energy values (Table 3) of simulated apoprotein structures show no major variation compared to the remaining X-ray structures. The

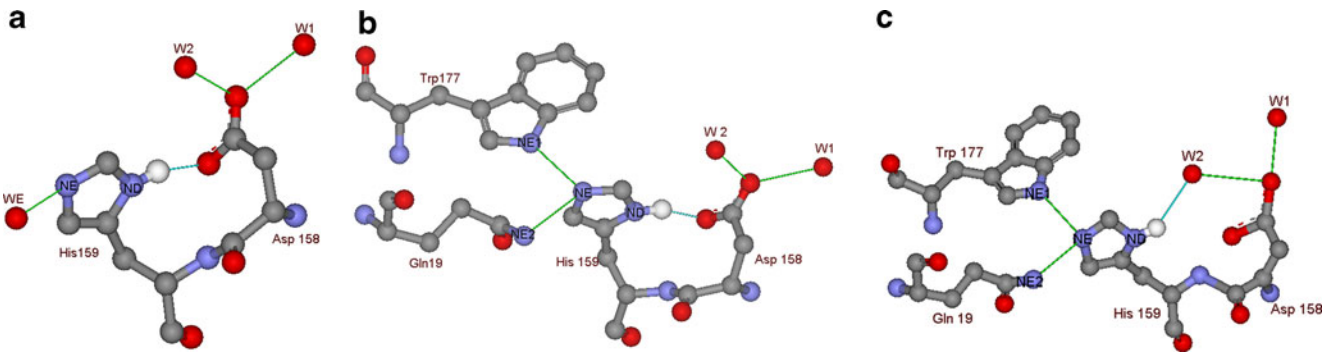

Fig. 3 **a** Dynamic conformation of complex IIᴵ (formed through the interaction of the His159 and Asp158 residues). **b** Dynamic conformation of complex II (formed through the interaction of the Gln19, His159, Asp158, and Trp177 residues) **c** Dynamic conformation of complex III (formed through the interaction of the Gln19, His159, Asp158, and Trp177 residues)

Table 3 Torsion angles (°) of the His159 and Asp158 side chains and the stability free energies (kcal mol^{-1}) of the plant thiol protease structures

Structure	Torsion angles of catalytic histidine		Torsion angles of the Asp158* side chain		Stability free energy
	χ_1 (X-ray/MD)	χ_2 (X-ray/MD)	χ_1 (X-ray/MD)	χ_2/χ_3 (X-ray/MD)	
1PPN	−174.41	51.26	90.53	16.15	90.53
	−76.58	**78.18**	**85.16**	**24.78**	**85.16**
9PAP	−170.70	60.10	106.82	20.26	106.82
	−78.97	**64.09**	**101.27**	**24.12**	**101.27**
1PE6	−169.10	47.61	103.75	16.53	103.75
	−91.09	**58.51**	**105.44**	**16.83**	**105.44**
1PPP	−176.89	63.04	189.20	2.54	189.20
	−91.55	**56.01**	**177.60**	**5.46**	**177.60**
1KHP	−178.10	53.97	95.15	24.11	95.15
	−80.85	**79.99**	**94.78**	**35.77**	**94.78**
1KHQ	−174.11	53.93	51.94	18.83	51.94
	−105.74	**77.46**	**64.98**	**15.64**	**64.98**
1BP4	−174.15	63.65	98.28	−4.30	98.28
	−101.98	**57.44**	**101.03**	**3.51**	**101.03**
1AEC	−174.43	64.85	58.31	7.40	58.31
	−76.23	**64.36**	**70.99**	**11.28**	**70.99**
2ACT	176.95	74.29	77.57	18.00	77.57
	−156.96	**−85.25**	**93.55**	**20.35**	**93.55**
1MEG	−175.10	62.57	99.67	64.68/-7.02	99.67
	−151.12	**−94.40**	**103.46**	**65.15/-3.08**	**103.46**
1YAL	−173.46	50.00	58.67	14.20	67.58
	−114.63	**66.47**	**58.40**	**18.63**	**79.44**
1CQD	−166.15	62.46	50.78	−133.41	110.88
	−125.01	**70.62**	**50.78**	**−133.41**	**119.18**
1IWD	−170.81	40.86	57.07	36.61	82.64
	−113.82	**64.45**	**57.07**	**38.68**	**84.95**
2BDZ	−176.90	47.43	67.56	−20.44	74.85
	−155.15	**−81.73**	**61.01**	**−31.24**	**87.46**
1GEC	−171.89	53.49	53.56	9.38	178.57
	−110.60	**63.84**	**54.41**	**14.62**	**179.00**
2PNS	−170.42	66.66	52.06	51.01	78.04
	−130.14	**67.99**	**52.06**	**42.00**	**86.67**

Nonbold values are for PDB structures; bold values are for MD-simulated structures

*Asp158 (1PPN, 9PAP, 1PE6, 1PPP, 1KHP, 1KHQ, 1BP4, 1YAL, 1GEC, 2BDZ), Asp161 (1AEC, 2ACT)/Glu158 (1MEG)/Asn157 (1IWD)/Asn156 (2PNS)/Asn160 (1CQD)

interaction between Trp177, Gln19, and the water molecule W_E at the NE2 site of the imidazole ring, and the participation of the WD_1, W_1, and W_2 hydrophilic sites with the carboxyl oxygen atom of Asp158 or the interaction with WD_1 and W_2 at ND1 of His159 may support the possible involvement of the different dynamic conformations I–II–II^I–III in the catalytic pathway of plant thiol protease (Figs. 2 and 3). The transition from I to III is observed in 1PE6, 1KHQ, and 1BP4, the I to II transition is observed in 2ACT, 1MEG, 1YAL, 1CQD, 1IWD, 2BDZ, and 1GEC, the transition from I to II^I is observed in 1PPN and 9PAP, and finally the transitions from I–II^I–II are observed in 1AEC, 1KHP, and 1PPP. The conformational stability free energy (ΔG) of the respective I, II, II^I, and III structural moieties (Fig. 2) are 0.41, 0.89, 1.14, and 2.50 kcal mol^{-1}, respectively. The WD_1, WD_2, and W_1 hydrophilic sites were found to be conserved in both the static and simulated X-ray structures. Hence, they may play an integral role in the catalytic process (Table 5).

Simulation studies of the solvated (CHASA) structures mostly revealed the interaction of a water molecule (the W_2 hydrophilic center) with ND1 of His159, although at ~55 ps the carboxyl oxygen atom of the catalytic Asp158 was observed to interact directly with the ND1 atom. The interactions of Trp177 and Gln19 with the NE2 atom of His159 were also observed in the solvated structures (Fig. 4a), and the corresponding distances are given in Table 6. This dynamic conformation supports structure III in Fig. 2. Again, during the simulation of the VMD-solvated 1PPN structure, a water molecule is consistently

Table 4 The residence times of different intermediate structures in a 2 ns MD simulation of plant thiol protease

PDB code	I	II′	II	III
1PPN	X-ray	0–2.0	–	–
9PAP	X-ray	0–2.0	–	–
1PE6	X-ray	–	–	0–2.0
1PPP	X-ray	0–0.8	0.8–2.0	–
1KHP	X-ray	0–0.6, 1.2–1.4, 1.6–2.0	0.6–1.2, 1.4–1.6	–
1KHQ	X-ray	–	–	0–2.0
1BP4	X-ray	–	–	0–2.0
1AEC	X-ray	0–0.6, 1.6–2.0	0.8–1.6	–
2ACT	X-ray	–	0–2.0[a]	–
1MEG	X-ray	–	0–2.0[a]	–
1YAL	X-ray	–	0–2.0[b]	–
1CQD	X-ray	–	0–2.0[b]	–
1IWD	X-ray	–	0–2.0[b]	–
2BDZ	X-ray	–	0–2.0[a]	–
1GEC	X-ray	–	0–2.0[b]	–
2PNS	X-ray	–	1.4–2.0[b]	–

[a]The ND1 atom interacts with the backbone oxygen atom of Ala160 (1MEG, 2BDZ)/Ala163 (2ACT)

[b]The ND1 atom interacts with the backbone oxygen atom of Asp158 (1YAL)/of Asn160 (1CQD)/Asn156 (2PNS)/ Asn157 (1IWD)/with the OG atom of Ser136 (1GEC)

observed to occupy the conserved hydrophilic center (W_E) and interact with the NE2 nitrogen atom of catalytic histidine (His159). However, at different time intervals, this position is also occupied by different water molecules (Table 6). At times, the hydrogen-bonding interaction between the conserved W_E center and another water center (whose position is mostly occupied by the low-occupancy water molecules W6121, W7274, W5659, W4250, W4613, W6521, W4613, W5967, W4361, W6341, and W7319) is also observed. The observation of a direct interaction between the acidic oxygen of Asp158 and ND1 of His159 (when W_E is bonded to the NE2 atom of histidine) in the simulated IPPN (VMD-solvated) structure may also support dynamic conformation II^I (Fig. 2) of the enzyme. However, for a short period, the simultaneous occurrence of water-mediated hydrogen bonding between the Asp158 and His159 (ND1) and an interaction between NE1 of Trp177 and NE2 of His159 in the structure of cysteine protease (Fig. 4b) may partially support the dynamic conformation III (Fig. 2).

Table 5 The water-mediated H-bonding interactions of catalytic His159 and Asp158 in X-ray and MD-simulated structures. The water molecules WD_1 and WD_2 form H-bonds with the ND1 atom of catalytic histidine, and the water molecules W_1 and W_2 H-bond with Asp158

PDB structures	X-ray structure							
	WD1	WD2	W 1	Residue that interacts with the NE2 atom of His	WD1	W1	W2	Residue or water molecule (W_E) that interacts with the NE2 atom of His
1PPN	W401 (38.14)	W309 (41.06)	W276 (21.40)	OD_1^{N175}	$OD1^{D158}$	–	–	W317
9PAP	W42 (24.02)	W43 (24.36)	W38 (20.83)	OD_1^{N175}	$OD1^{D158}$	W38	W97	W42
1PE6	W234 (42.54)	$O18^{E6C}$ (23.25)	W408 (25.29)	OD_1^{N175}	–	W 408	W 234	$NE2^{Q19}/NE1^{W177}$
1PPP	$O18^{E6C}$ (23.14)	W287 (22.44)	W372 (37.29), W387 (16.92)	OD_1^{N175}	$OD1^{D158}$	W372	W387	$NE2^{Q19}/NE1^{W177}$
1KHP	CM^{GLM} (31.47)	W317 (43.82)	W320 (43.96)	OD_1^{N175}	$OD1^{D158}$	W320	–	W317
1KHQ	W350 (46.49)	W379 (38.91)	W344 (34.52)	OD_1^{N175}	–	W344	W379	$NE2^{Q19}/NE1^{W177}$
1BP4	$O34^{ALD}$ (49.3 4)	–	W446 (24.76)	OD_1^{N175}	–	W446	W412	$NE2^{Q19}/NE1^{W177}$
1AEC	W426 (38.39)	$O1^{E64}$ (10.30)	W71 (13.86)	$OD1^{N175}$	$OD1^{D161}$	W71	W220	W193
2ACT	W437 (50.00)	W298 (28.18)	W71 (27.01)	OD_1^{N182}	–	W71	W214	$NE2^{Q19}/NE1^{W184}$
1MEG	O1E64 (8.07)	W310 (13.13)	OG^{S136} (8.94)	OD_1^{N179}	–	OG^{S136}	–	$NE2^{Q19}/NE1^{W181}$
1YAL	SG^{SCH} (15.61)	W424 (59.04)	W16 (24.39)	OD_1^{N179}	–	W16	W108	$NE2^{Q19}/NE1^{W181}$
1CQD	$S2^{THJ}$ (44.68)	–	OD_1^{D137} (24.39)	OD_1^{N181}	–	–	–	$NE2^{Q21}/NE1^{W183}$
1IWD	$S2^{THJ}$ (27.63)	W442 (38.51)	W414 (34.79)	OD_1^{N178}	–	W414	W412	$NE2^{Q19}/NE1^{W180}$
2BDZ	$O2^{E64}$ (12.19)	W1132 (18.62)	OG^{S136} (9.90)	OD_1^{N175}	–	W1132	–	$NE2^{Q19}/NE1^{W177}$
1GEC	CM^{GLM} (17.70)	W235 (10.17)	W293 (21.89)	OD_1^{N179}	OG^{S136}	W293	W257	$NE2^{Q19}/NE1^{W181}$
2PNS	O_1^{THJ} (95.69)	W720 (43.43)	–	OD_1^{N173}	–	–	–	$NE2^{Q19}/NE1^{W175}$

* *B* factors of the respective atoms or water molecules are given in parentheses

Table 6 The side-chain interaction of catalytic histidine with water molecules and other residues in the (CHASA- and VMD-solvated) MD-simulated 1PPN structure

Snapshots (in ns)	Interaction with the NE2 atom of catalytic histidine (VMD) (W_E)	Interaction with the NE2 atom of catalytic histidine (CHASA)	Interaction with the ND1 atom of catalytic histidine (CHASA) (W_2)
0.1	W7405 (2.91)	R_W/R_Q (2.95)/(3.28)	W 229 (3.13)
0.2	W5113 (2.87)	R_W/R_Q (3.05)/(3.79)	W 229 (3.56), R_D (3.14)
0.3	W5113 (2.92)	R_W/R_Q (2.93)/(3.72)	W 229 (3.38), W292 (3.09)
0.4	W7274 (2.92)	R_W/R_Q (5.21)/(5.31)	W 244 (3.18), R_D (2.75)
0.5	W4613 (3.19)	R_W/R_Q (2.99)/(4.41)	W 229 (2.94)
0.6	W6960 (2.90)	R_W/R_Q (3.17)/(3.25)	W 229 (3.21)
0.7	W4613 (3.28)	R_W/R_Q (3.22)/(3.68)	W 229 (3.02)
0.8	W7274 (3.02)	R_W/R_Q (3.22)/(3.48)	W 227 (2.82)
0.9	W6521 (2.91)	R_W/R_Q (3.44)/(3.67)	W 227 (2.64)
1.0	W2989 (3.00)	R_W/R_Q (2.88)/(3.83)	W 227 (2.89)
1.1	W5367 (3.09)	R_W/R_Q (3.32)/(4.35)	W 244 (3.13), R_D (3.14)
1.2	W4361 (2.79)	R_W/R_Q (3.08)/(4.33)	W 243 (2.86)
1.3	W5184 (2.90)	R_W/R_Q (3.08)/(4.24)	W 243 (3.04)
1.4	W4930 (2.75)	R_W/R_Q (3.11)/(3.86)	W 385 (3.01)
1.5	W4930 (3.28)	R_W/R_Q (2.93)/(4.37)	W 385 (3.28)
1.6	W7022 (3.12)	R_W/R_Q (2.87)/(3.92)	W 385 (2.79)
1.7	W7022 (3.08)	R_W/R_Q (2.91)/(3.34)	W 385 (3.05)
1.8	W6.55 (2.77)	R_W/R_Q (2.90)/(3.20)	W 385 (2.95)
1.9	W5948(3.29)	R_W/R_Q (3.18)/(3.36)	W 385 (2.85)
2.0	W4755 (2.95)	R_W/R_Q (2.86)/(4.23)	W 385 (3.00)

* The distances (Å) are given in parentheses

R_D Asp158 (OD1 atom)

R_W Trp177 (NE1 atom)

R_Q Gln19 (NE2 atom)

Thus, these results support the hydrophilic susceptibility of the NE2 and ND1 atoms of catalytic His159 and the OD1 atom of Asp158. During the simulation of the plant thiol protease structures, the intricate hydrogen-bonding interactions of the water molecule W_E with NE2, WD_1 and W_2 with ND1, and W_1 and W_2 with Asp158 (OD1) appear to be interesting. Moreover, the interaction of the carboxyl oxygen (OD1) of Asp158 with the ND1 atom of His159, and interactions of both the Trp177 (NE1), Gln19 (NE2) residues with the NE2 atom of His159 have also been observed during the dynamics. However, the occupation frequencies of these water molecules seem to differ, which may be due to their high *B* factors or mobility in the X-ray structures. The ND1-bound WD_1 and WD_2 hydrophilic centers are conserved in the X-ray structures, but the WD_1 nearly retains its position during simulation, while the water molecule at WD_2 is moved to about ~4.5 Å. Again, due to the transition of the dynamic structure from I to III in Fig. 2, the interactions of water molecules at two nitrogen centers of the His159 imidazole ring and the carboxyl oxygen of Asp158 also vary with time. Interestingly, the hydrophilic positions WD_1 and W_2 near the ND1 atom appear to be conserved. However, these sites are mostly occupied by different water molecules at different times. Similarly, the Asp158 (OD1)-bound W_2 hydrophilic position is also thought to be conserved in some structures. The

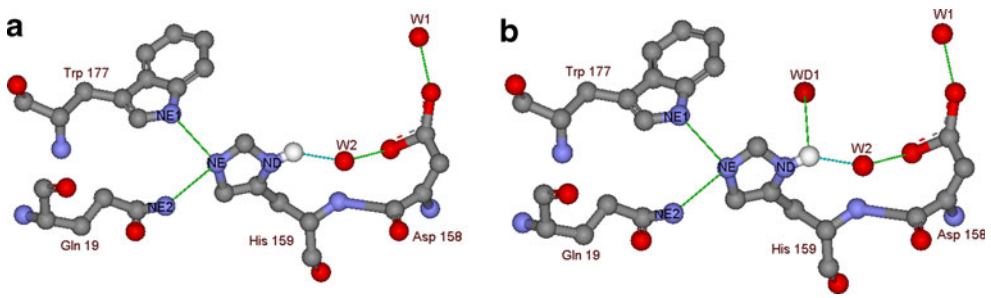

Fig. 4 **a** The water-mediated interaction in the CHASA-solvated 1PPN structure during dynamics. **b** The water-mediated interaction in the VMD-solvated 1PPN structure during dynamics

occasional occurrence of the Asp158 (OD1) oxygen atom at the hydrophilic WD_1 site also indicates the conserved character of the WD_1 position. The W_E position is occupied by different water molecules at different times, but this hydrophilic W_E site also appears to be conserved during the lifetime of structure II, particularly in the VMD-solvated structures. Therefore, the hydrophilic centers WD_1, W_1, W_2, and W_E are conserved in one or more of the dynamic conformations I–III (Fig. 2), though some of the water centers may not be conserved over the entire period of simulation.

Conclusions

The results obtained so far for all of the apo structures of plant thiol protease highlight the roles played by some water molecules in the coupling of His159 and Asp158 residues. The interaction of His159 with WD_1 and WD_2 and the interaction of Asp158 and W_1 are conserved in all of the X-ray structures. During simulation, the conserved hydrophilic W_1, W_2, and WD_1 water centers form hydrogen bonds with Asp158 (OD1) and His159 (ND1). In some VMD-solvated structures, the hydrophilic center (W_E) was also found to be conserved. Therefore, we can assume that these conserved hydrophilic centers play a critical role in the formation, stabilization, and transitions of His–Asp hydrogen-bonded complexes in the catalytic zone of the enzyme. During the absence of the water-mediated interaction at ND1, the OD1 (Asp158) atom appears to form a direct hydrogen bond with the imidazole nitrogen atom of His159. In the absence of the water-mediated (W_E) interaction at the NE2 site, the Trp177 (NE1) and Gln19 (NE2) residues influence the NE2 atom of His159. In both the X-ray and solvated protein structures, the stereoselective recognition between His159 and Asp158 is thought to be influenced by water molecules. Therefore, conserved water molecules may play an important role in the catalytic activity of plant thiol protease. A few dynamic conformations or transition states involving direct and water-mediated His–Asp hydrogen-bonded complexes are envisaged from these studies.

Acknowledgments We thank and acknowledge the National Institute of Technology Durgapur for providing a research facility in the Department of Chemistry. We also thank and acknowledge Dr. K Sekar, Indian Institute of Science, Bangalore, India, for critically reading this manuscript.

References

1. Otto HH, Schirmeister T (1997) Chem Rev 97:133–171
2. Komatsu K, Tsukuda K, Hosoya J, Satoh S (1986) Exp Neurol 93:642–646
3. Sloane BF, Moin K, Krepela E, Rozhin J (1990) Cancer Metastasis Rev 9:333–352
4. Lecaille F, Kaleta J, Bromme D (2002) Chem Rev 102:4459–4488
5. Huet G, Flip RM, Richet C, Thiebet C, Demeyer D, Balduyck M, Duquesnoy B, Degand P (1992) Clin Chem 38:1694–1697
6. Polgár L (1974) FEBS Lett 47:15–18
7. Vernet T, Tessier DC, Chatellier J, Plouffe C, Lee TS, Thomas DY, Storer AC, Menard R (1995) J Biol Chem 270:16645–16652
8. Harrison MJ, Burton NA, Hillier IH (1997) J Am Chem Soc 119:12285–12291
9. O'Farrell PA, Joshua-Tor L (2007) Biochem J 401:421–428
10. Mladenovic M, Fink RF, Thiel W, Schirmeister T, Engels B (2008) J Am Chem Soc 130:8696–8705
11. Nandi TK, Bairagya HR, Mukhopadhyay BP, Sekar K, Sukul D, Bera AK (2009) J Biosci 34:27–34
12. Menard R, Khouri HE, Plouffe C, Laflamme P, Durpras R, Vernet T, Tessier DC, Thomas DY, Storer AC (1991) Biochemistry 30:5531–5538
13. Wang J, Xiang YF, Lim C (1994) Protein Eng Des Sel 7:75–82
14. Dijkman JP, Van Duijnen PTh (1991) Int J Quant Chem 40:49–59
15. Welsh WJ, Lin Y (1997) J Mol Struct THEOCHEM 401:315–326
16. Day RM, Thalhauser CJ, Sudmeier JL, Vincent MP, Torchilin EV, Sanford DG, Bachovchin CW, Bachovchin WW (2003) Protein Sci 12:794–810
17. Berman HM, Westbrook J, Feng Z, Gilli G, Bhat TN, Weissig H, Shindyalov IN, Bourne PE (2000) Nucleic Acids Res 28:235–242
18. Pickersgill RW, Harris GW, Garman E (1992) Acta Crystallogr Sect B 48:59–67
19. Kamphuis IG, Kalk KH, Swarte MB, Drenth J (1984) J Mol Biol 179:233–256
20. Yamamoto D, Matsumoto K, Ohishi H, Ishida T, Inoue M, Kitamura K, Mizuno H (1991) J Biol Chem 266:14771–14777
21. Kim MJ, Yamamoto D, Matsumoto K, Inoue M, Ishida T, Mizuno H, Sumiya S, Kitamura K (1992) Biochem J 287:797–803
22. Janowski R, Kozak M, Jankowska E, Grzonka Z, Jaskolski M (2004) J Pept Res 64:141–150
23. LaLonde JM, Zhao B, Smith WW, Janson CA, DesJarlais RL, Tomaszek TA, Carr TJ, Thompson SK, Oh HJ, Yamashita DS, Veber DF, Abdel-Meguid SS (1998) J Med Chem 41:4567–4576
24. Varughese KI, Su Y, Cromwell D, Hasnain S, Xuong NH (1992) Biochemistry 31:5172–5176
25. Baker EN, Dodson EJ (1980) Acta Crystallogr Sect A 36:559–572
26. Katerelos NA, Taylor MA, Scott M, Goodenough PW, Pickersgill RW (1996) FEBS Lett 392:35–39
27. Maes D, Bouckaert J, Poortmans F, Wyns L, Looze Y (1996) Biochemistry 35:16292–16298
28. O'Hara BP, Hemmings AM, Buttle DJ, Pearl LH (1995) Biochemistry 34:13190–13195
29. Biswas S, Chakrabarti C, Kundu S, Jagannadham MV, Dattagupta JK (2003) Proteins 51:489–497
30. Ghosh R, Dattagupta JK, Biswas S (2007) Biochem Biophys Res Commun 362:965–970
31. Choi KH, Laursen RA, Allen KN (1999) Biochemistry 38:11624–11633
32. Guex N, Diem A, Peitsch MC, Schwede T (2001) The deep view—the Swiss-PdbView program, an environment for comparative protein modeling. GlaxoSmithKline R&D, London
33. Humphrey W, Dalke A, Schulten K (1996) J Mol Graph 14:33–38
34. Brooks BR, Bruccoleri RE, Olafson BD, States DJ, Swaminathan S, Karplus M (1983) J Comput Chem 4:187–217
35. Nelson M, Humphrey W, Gursoy A, Dalke A, Kale L, Skeel RD, Schulten K (1996) Int J Supercomput Appl High Perform Comput 10:251–268
36. Phillips JC, Braun R, Wang W, Gumbart J, Emad Tajkhorshid E, Villa E, Chipot C, Skeel RD, Kale L, Schulten K (2005) J Comput Chem 26:1781–1802

37. Fleming PJ, Nicholas C, Fitzkee MM, Rajgopal S, George DR (2005) Protein Sci 14:111–118
38. Bairagya HR, Mukhopadhyay BP, Sekar K (2009) J Bio Struct Dyn 26:497–507
39. Bairagya HR, Mukhopadhyay BP, Sekar K (2009) J Bio Struct Dyn 27:149–158
40. Schymkowitz J, Borg J, Stricher F, Nys R, Rousseau F, Serrano L (2005) Nucleic Acids Res 33:382–388
41. Mustata G, Briggs JM (2004) Protein Eng Des Sel 17:223–234
42. Gul S, Hussain S, Thomas MP, Resmini M, Verma CS, Thomas EW, Brocklehurst K (2008) Biochemistry 47:2025–2035
43. Stollar EJ, Gelpi JL, Velankar S, Golovin A, Orozco M, Luisi BF (2004) Proteins 57:1–8
44. Sulpizi M, Rothlisberger U, Carloni P (2003) Biophys J 84:2207–2215